공학 석사 학위 논문

Temperature-dependent shear correction factors for thermal-structural stability of step-wise FGM panel with micromechanical properties

미소기계적 물성을 가진 층 경사기능재료의 온도 의존 전단보정계수와 열적 구조 안정성 연구

2017 년 8 월

서울대학교 대학원

기계항공공학부

임 태 경

Abstract

As advanced structures, Functionally Graded Materials (FGMs) have been used in high temperature regions for aerospace, automobile, and commercial structures et al. In this regard, present study investigated thermo-elastic vibration and post-buckling behaviors for the FGMs model. And thermo-micromechanical modified shear correction factors are used for crucial evaluation to compensate the shear stress effects in thermal environments. Layer-wise modeled FGMs plates are investigated in the thermo-mechanical environment and it is more actual method to approach FGMs analysis. For the thermal-structural analysis, First-order Shear Deformation Theory of Plate (FSDTP) is employed with thermo-micromechanical properties. And, the materials are based on the power law distribution in the thickness direction of the model. Especially, the materials have non-homogeneous properties with varying gradually from one surface to the other. Material properties are assumed to be temperature dependent and neutral surface is adopted reference plane due to of asymmetry of the material properties in the thickness direction, because the mid-plane of the FGMs plate model is not equal to the neutral surface of the structure. Homogenization modeling of FGMs plates is investigated in the thermo-mechanical environment, and it is more actual method to approach FGMs analysis. In this regard, Mori-Tanaka Scheme (MTS) explicitly evaluates particle interactions, and the governing formulation is based on FSDTP and the von Karman strain-displacement equation to consider geometric nonlinearity. Furthermore, Newton-Raphson method is applied solve the thermal post-buckling analysis. In order to

validate analyses, results are compared with previous data of continuous FGMs model. The influence of homogenized model and neutral surface on the thermo-elastic analysis of FGMs is also highlighted.

Key words : FGMs plate, Shear correction factor, Neutral surface, Vibration, Thermal post-buckling, Mori-Tanaka scheme

Student Number : 2015-22737

Contents

List of Table and Figure

Tables

Figures

List of Nomenclature

A	In-plane stiffness matrix
A_d	Aerodynamic damping matrix
A_f	Aerodynamic influence matrix
A_s	Transverse shear stiffness
a	Plate length
B	In-plane bending coupling stiffness matrix
$B(z,T)$	Bulk modulus
b	Plate width
C_R	Reduced damping matrix
D	Bending stiffness matrix
d	Displacement vector
E	Young's modulus
f	External force vector
$G(z,T)$	Shear modulus
h	Plate thickness
K	Linear elastic stiffness matrix
$K(z,T)$	Heat conductivity
$K_{\Delta T}$	Thermal stiffness matrix
K_R	Reduced stiffness matrix
k	Volume fraction index
k_T	Temperature-dependent Shear correction factor
M	Mass matrix
$M_b, M_{\Delta T}$	Moment resultant and thermal moment resultant, respectively
M_R	Reduced mass matrix
$N_b, N_{\Delta T}$	In-plane force resultant and thermal in-plane force resultant, respectively
$N1, N2$	First-order non-linear stiffness and second-order non-linear stiffness matrices, respectively
P, P_{eff}	Material property and effective material property

$P_{\Delta T}{}^{*}$	Thermal load vector
Q_s	Transverse shear force resultant vector
$T,$	Temperature
T_i, T_f	Reference temperature and final temperature, respectively
ΔT	Temperature elevation
u	In-plane displacement in the x direction
v	In-plane displacement in the y direction
V	Volume fraction
w	Transverse displacement in the z direction
z_0	Neutral surface shift
$\partial W_{\text{int}}, \partial W_{ext}$	Internal and external virtual
α	Thermal expansion coefficient
λ	Non-dimensional aerodynamic pressure
ϕ_x, ϕ_y	Rotation of the normal in the xz and yz plane, respectively
φ_0	Time independent vector
ω	Plate motion parameter
ρ	density of ring material
σ	stress

Subscripts

cr	Critical
c	Ceramic
m	Metal
n	Number of layer
s	Static state
t	Dynamic state

1. Introduction

Composite material is defined as a combination of two or more distinct materials to create a new material with the properties. It can be determined that a wide range of engineering situation. Functionally Graded Materials (FGMs) have been developed with substantial importance with the durability in extremely high temperatures, and are commonly used in the surface structures of spacecraft and military missions. The materials are usually made up of the gradual mixture of ceramic and metal in the thickness direction of the structures. The concept of FGMs was originated in mid-1980 in Japan during a space plane project in which a combination of materials was used to act as thermal barrier. [1] Since the material compositions of FGMs are varied gradually from a materials to another one, those interface problems can be effectively reduced. [2]

FGMs have been emerged from manufacturing a composite material in high temperature status. Specially, FGMs are made of the continuous mixture of ceramic and metal and the material properties have smooth and continuous pattern from one surface to the other as compared with conventional composite, and ceramic has high compressive strength and heat resistance with low fracture toughness, but metal exhibits better mechanical strength while cannot withstand at high thermal environment. These attractive merits have increased the roles of FGMs in various engineering fields. In particular, FGMs plate made of a ceramic and a metal can be used as an outer wall of a space model which is subjected to high temperature changes. In this case, when the model flies under high thermal environments, the plates can be experience serious structural problems, such as thermal vibration or buckling.

Therefore, it is necessary to study the temperature-dependent modeling and analysis of FGMs plates to ensure reliable design.

For about three decades, research works of thermal buckling and post-buckling on the materials have been investigated. Bouazza et al.[3] studied the thermo-elastic buckling behavior of structures based on First-order Shear Deformation Theory of Plate (FSDTP). Furthermore, Bouiadjra et al.[4] analyzed the thermal buckling behavior of the model using a refined plate theory. And then, S. R. Li et al. [5] presented analysis of thermal post-buckling of FGMs Timoshenko beams subjected to transversely non-uniform temperature rise. Prakash et al. [6] investigated the post-buckling behavior of FGM skew plate under thermal load based on shear deformable finite element approach. Shen [7] reported thermal post-buckling analysis for a simply supported, shear deformable FGMs plate under thermal loading. Lee and Kim [8] studied the supersonic aero-thermo post-buckling behaviors and limit-cycle oscillations of FGM panels using Newmark's time integration method. Lee and Kim [9] performed the thermo-mechanical behavior of FGM panels in hypersonic airflows. Achchhe Lal et al. [10] examined the second-order statistics of post-buckling of FGM subjected to mechanical and thermal loading with non-uniform temperature changes subjected to temperature independent and dependent material properties. Liew et al. [11] presented thermal buckling and post-buckling analysis for moderately thick laminated rectangular plates that contain FGMs and subjected to a uniform temperature change.

Recently, as the use of FGMs plates for space models is expected to increase, researches on dynamic characteristics and stability of FGMs plate

are being performed. Navazi and Haddapour [12] determined the aero-thermoelastic stability margins of FGM plates using analytical approach. Sohn and Kim [13] investigated static and dynamic stabilities of FGM panels which are subjected to combines thermal and aerodynamic loads. Prakash and Ganapathi [14] investigated the influence of thermal environment on the supersonic flutter behavior of flat plates made of functionally graded materials using finite element procedure. Lee et al. [15] performed flutter analysis of stiffened laminated plates to analyze the dynamic characteristics of stiffened plates subjected to thermal load. Ibrahim et al. [16] studied the non-linear flutter and thermal buckling of FGM panels under the combined effect of elevated temperature conditions and aerodynamic loading. Haddapour et al. [17] revealed the nonlinear aeroelastic behavior of FGM plates in supersonic flow.

For equilibrium of structure, neutral surface has been used as a reference plane due to the asymmetry of material properties in the thickness direction of FGMs as compared with the previous works. Prakash and Singha [18] studied nonlinear behavior of FGMs skew plates under in-plane load. Zhang [19] considered a higher-order shear deformation theory of the plate models for thermal buckling behavior using the neutral concept. Yaghoobi and Fereidoon [20] indicated the influence of neutral surface position on deflection.

However, these research works considered only in the macroscopic material properties of FGMs, and more reliable data for the structure can be obtained using micromechanical level estimation of the properties. Mori and Tanaka [21] originally concerned with an estimation of the average internal stress in matrix of a material containing precipitates with eigen-strains for composite

materials. Therefore, numerous analysis of homogenized FGMs are studied in various environments. Shen and Wang [22] considered the small and large amplitude vibration for a FGMs plates resting in a two-parameter elastic foundation in thermal environments. Kiani and Eslami [23] investigated thermal post-buckling of solid circular plates made of a through-the-thickness FGMs on three different homogenization schemes. Akabarzadeh et al. [24] examined the influence of alternative micro-mechanical models on the macroscopic behavior of a FGMs plate based on classical and shear-deformation plate theories.

Practical point of view, the transverse shear stress is assumed to be constant through the thickness direction in the FSDTP. And thus, the shear correction factor is considered to compensate the numerical error of the model. In this regard, Stefanos [25] commented the importance of the correction factors for plates and shells. Also, Madabhusi-Raman and Davalos [26] studied the static shear correction factor for composite material. Furthermore, Birman and Bert [27] reviewed the methods to determine the factor for sandwich plates. While, Nguyen and Sab [28] performed stress analysis of FSDTP model using the modified shear correction factor. Recently, Menaa et al. [29] obtained the analytical solutions for static correction factor of rectangular beam models. For a more improved analysis in thermal environments, Lim and Kim [30] suggested thermo-elastic shear correction factors of the beam structure. Furthermore, Lim and Kim [31] proposed thermo-micromechanically modified shear correction factors to consider the properties in micromechanical level.

In this paper, thermal post-buckling and limit-cycle oscillation characteristics of FGMs plate are studied based on neutral surface using homogenization method. The plates are considered as temperature dependent model in thermal environments, and models are assumed as plates based on the first-order shear deformation theory. Material properties of the plates with temperature dependent are continuously varied in the thickness direction, and adopted micro-mechanical characteristic. For the microscopic modeling of the structure, Mori-Tanaka Scheme (MTS) is employed for more accurate estimation of material properties. Also, aim of present study is to use the neutral surface concept, and the results compares the post-buckling and limit-cycle oscillation characteristics with the previous data based on conventional reference plane. In order to discuss the present works, the cases of models are considered with and without heat conduction effects in the thickness direction.

2. Formulation

Fig. 1 shows the layer-wise FGMs plate model and precisely the material properties in the thickness direction are asymmetric. The structure with the mixture of ceramic and metal and the structure has the length, width and thickness as L, b, h, respectively. In this work, the formulation is based on the First-order Shear Deformation Theory of Plate (FSDTP) including the heat transfer effects.

2.1. Functionally graded materials

Generally, the Power-law (P-), Exponential (E-) and Sigmoid (S-) FGM models are commonly used in order to define the volume fractions for three types of material models. Specifically, FGMs are designed to be suitable for high-temperature status, thus temperature-dependency of the material characteristics is a significantly important topic for the models.

Then, the material properties $P(T)$ can be expressed as in Ref. [32].

$$P(T) = P_0(P_{-1}T^{-1} + 1 + P_1T + P_2T^2 + P_3T^3) \tag{1}$$

where T denotes the temperature of the material, and P_0, P_{-1}, P_1, P_2 and P_3 stand for the constants in the cubic fit of the material properties.

Firstly, P-FGM model is defined as a mixture of ceramics and metals, and then the mixture ratio varies continuously and smoothly in the thickness direction.

The rule of mixture (ROM) is adopted, and then, the properties can be written as:

$$V_{cn}(z_n)=\left(\frac{z_n}{h}+\frac{1}{2}\right)^k \quad (0\le k<\infty),\ V_{cn}(z)+V_{mn}(z)=1\ (n:\text{Number of layer}) \tag{2}$$

in here k , V_c , and V_m represent the volume fraction index, the volume fractions of ceramic and metal, respectively. From now on, the metal- and ceramic-rich surfaces are defined as the bottom and top surfaces, respectively.

Considering Eqns. (1) and (2), the effective material properties at z can be expressed as:

$$\begin{aligned} P_{\text{eff,n}}(z,T) &= P_m(T)V_{mn}(z)+P_c(T)V_{cn}(z) \\ &= P_m(T)+(P_c(T)-P_m(T))\left(\frac{z_n}{h}+\frac{1}{2}\right)^k \end{aligned} \tag{3}$$

where h and P represent the thickness of the plate model. Additionally, subscript *eff* indicates the effective of all the properties such as Young's modulus, thermal expansion coefficient, thermal conductivity and Poisson's ratio.

Next, the E-FGM model is used to describe the material properties by many researchers with a constant value irrespective of the volume fractions.

$$P_{eff,n}(z,T) = Ae^{B(z_n+h/2)} \qquad \text{in here,} \quad A = P_m,\ B = \frac{1}{h}\ln\left(\frac{P_c}{P_m}\right) \tag{4}$$

Finally, S-FGM is proposed in order to reduce the stresses concentrations as compared with the P- and E- models as in Ref. [1]. Also, this model makes sure that the stresses have a more smooth distribution than P- type model.

Then, the volume fraction is expressed as:

$$V_{cn}(z_n) = \begin{cases} V_{cn1} = 1 - \dfrac{1}{2}\left(1 - \dfrac{2z_n}{h}\right)^k & (0 \le z \le h/2) \\ V_{cn2} = \dfrac{1}{2}\left(1 + \dfrac{2z_n}{h}\right)^k & (-h/2 \le z \le 0) \end{cases} \tag{5}$$

In this case, effective material properties can be obtained by a linear rule of mixture:

$$\begin{aligned} P_{\text{eff,n}}(z,T) &= P_c(T)V_{cn1}(z) + P_m(T)(1 - V_{cn1}(z)) \qquad (0 \le z \le h/2) \\ P_{\text{eff,n}}(z,T) &= P_c(T)V_{cn2}(z) + P_m(T)(1 - V_{cn2}(z)) \qquad (-h/2 \le z \le 0) \end{aligned} \tag{6}$$

The mixture ratio and the effective material properties of the plate models vary continuously and smoothly through the thickness direction for Young's modulus E, Poisson's ratio ν, shear modulus G and mass density ρ.

2.2. Homogenization scheme

Mori and Tanaka [21] originally concerned with an estimation of the average internal stress in matrix of a material containing precipitates with eigen-strains for composite materials. In this regard, the present work reconsiders the application of the Mori-Tanaka Scheme (MTS) to the calculation of effective properties of materials. The previous method is easy to use, but it does not account for the interaction among adjacent inclusions and also evaluate approximate values of the effective elastic modulus. In other words, the method proposes the simple relations to find the bulk modulus and the shear modulus of the equivalent homogenized medium. Bulk modulus is defined as the ratio of the infinitesimal pressure increase to the resulting relative decrease of the volume. The locally effective bulk modulus $B(z,T)$ and shear modulus $G(z,T)$ of the temperature-dependent FGMs can be written as in Ref. [6].

$$\frac{B(z,T)-B_m(T)}{B_c(T)-B_m(T)}=\frac{V_c(z)}{1+[1-V_c(z)]\left[\dfrac{3B_c(T)-3B_m(T)}{3B_m(T)+4G_m(T)}\right]} \tag{7}$$

$$\frac{G(z,T)-G_m(T)}{G_c(T)-G_m(T)}=\frac{V_c(z)}{1+[1-V_c(z)]\left[\frac{G_c(T)-G_m(T)}{G_m(T)+f_1(T)}\right]} \tag{8}$$

In Eq. (5), $f_1(T)$ is defined as follows:

$$f_1(T)=\frac{G_m(T)[9B_m(T)+8G_m(T)]}{6[B_m(T)+2G_m(T)]} \tag{9}$$

Based on these formulas, Elasticity modulus, Poisson's ratio, thermal expansion coefficient and thermal conductivity are calculated.

For Young's modulus E is given by [22]:

$$E(z,T)=\frac{9B(z,T)G(z,T)}{3B(z,T)+G(z,T)} \tag{10}$$

Poisson's ratio ν is expressed as [22]:

$$\nu(z,T)=\frac{3B(z,T)-2G(z,T)}{2(3B(z,T)+G(z,T))} \tag{11}$$

The coefficient of thermal expansion α is determined from the relation [34]:

$$\frac{\alpha(z,T)-\alpha_c(T)}{\alpha_m(T)-\alpha_c(T)}=\frac{\dfrac{1}{K(z,T)}-\dfrac{1}{K_c(T)}}{\dfrac{1}{K_m(T)}-\dfrac{1}{K_c(T)}} \tag{12}$$

Next, the effective heat conductivity $K(z,T)$ is given by [35]:

$$\frac{K(z,T)-K_m(T)}{K_c(T)-K_m(T)}=\frac{V_c(z)}{1+[1-V_c(z)]\left[\dfrac{K_c(T)-K_m(T)}{3K_m(T)}\right]} \tag{13}$$

2.3. Physical neutral surface

As a reference plane for the force equilibrium of FGMs model, the neutral surface concept is to follow due to the asymmetry in the thickness direction of Young's modulus of materials. The neutral surface is an axis in the cross section of plates along which there are no longitudinal stresses or strains. If the section is symmetric, midpoint of isotropic model is not curved before a bend occurs, then the neutral surface is at the geometric centroid, but the neutral surface of FGMs is not same as mid-surface.

To determine the location of the neutral surface with the thermal effects, let the integration in the thickness direction for the first moment of elasticity modulus $E(z,T)$ equal to zero.

$$\sum_{n=1}^{N} E_n(z_n,T)\left(z_n - z_0(T)\right)\frac{z_n}{h} = 0 \tag{14}$$

Thus, the position of neutral surface for the layer-wise model $z_{0n}(T)$ can be obtained as [33]:

$$z_{0n}(T) = \frac{\sum_{n=1}^{N} E_n(z_n,T) z_n \frac{z_n}{h}}{\sum_{n=1}^{N} E_n(z_n,T)\frac{z_n}{h}} \tag{15}$$

As shown in this formula, z_0 is temperature-dependent because the Young's modulus changes due to temperature effects in the thickness direction.

Specially, For the P- E- and S-FGM models, non-dimensional neutral surface positions are obtained as follows by using Eq. (15). For P-FGM model:

$$\frac{z_{0n}(T)}{h} = \frac{k\left(E_c(T) - E_m(T)\right)}{2(k+2)\left(kE_m(T) + E_c(T)\right)} \tag{16a}$$

Next, for the case E-FGM:

$$\frac{z_0(T)}{h} = \frac{r(\frac{1}{2}\ln r - 1) + \frac{1}{2}\ln r + 1}{(r-1)(\ln r)} \quad \text{where } r = \frac{E_c(T)}{E_m(T)} \tag{16b}$$

Finally, for S-FGM model:

$$\frac{z_0(T)}{h} = \frac{k(k+3)(E_c(T) - E_m(T))}{4(k+1)(k+2)(E_c(T) + E_m(T))} \tag{16c}$$

2.4. Thermo-elastic shear correction factor

For the First-order Shear Deformation Theory of Plate (FSDTP), the model assumes to have a constant shear stress resultant. On the other hand, Ref. [28] obtained variable shear correction factors in order to consider the distribution of shear correction factors in the structures. For rigorous estimation of shear stress in the thermal-structural analysis, temperature-dependent shear correction factor is proposed in this work. Based on the previous work in Ref. [30], the moments, strains and stiffnesses of the plate model:

$$\begin{Bmatrix} \{N_T\} \\ \{M_T\} \end{Bmatrix} = \begin{bmatrix} [A_T] & [B_T] \\ [B_T] & [D_T] \end{bmatrix} \begin{Bmatrix} \{\varepsilon_T\} \\ \{\chi_T\} \end{Bmatrix} \tag{17}$$

where subscript T denotes temperature to present the temperature-dependent variables. Also, the stiffness matrix *A, B, D* of the plate model adopting the neutral surface concept:

$$(A_{\alpha\beta\gamma\delta}, B_{\alpha\beta\gamma\delta}, D_{\alpha\beta\gamma\delta})_T = \int_{-h/2}^{h/2} \left(1, (z - z_0(T)), (z - z_0(T))^2\right) C_{\alpha\beta\gamma\delta}(z) dz \quad (18)$$

Furthermore, shear forces are related to the average shear strains by the corresponding stiffness,

$$\begin{Bmatrix} Q_y \\ Q_x \end{Bmatrix}_T = \begin{bmatrix} H_{44} & H_{45} \\ H_{45} & H_{55} \end{bmatrix}_T \begin{Bmatrix} \gamma_{yz}^o \\ \gamma_{xz}^o \end{Bmatrix}_T \quad (19)$$

in here H_{ij} (i,j =4, 5) are the temperature-dependent shear stiffness. While, H_{45}=0 and H_{44}=H_{55} due to there is no coupling between the shear deformations in two directions. Thus the constitutive relation for transverse shear stress resultant:

$$\gamma_{xz}^o(T) = \left[\frac{Q_x}{H_{55}}\right]_T \quad (20)$$

Finally, the temperature-dependent shear correction factors for layer-wise plate are obtained as:

$$k_{55}(T) = \left(\sum_{n=1}^{N} S_{55}(z_n, T)\frac{z_n}{h}\right) H_{55}(z, T) \quad (21)$$

where, the transverse shear modulus at location z is:

$$S_{55} = \frac{2\left(1+\nu(z_n,T)\right)}{E(z_n,T)} \tag{22}$$

It is interesting that this formula is similar as the case in Ref. [28]. However, the present work considers the concept of neutral surface and also temperature-dependency.

3. Governing equations

3.1. Heat conduction

Considering a FGMs plate at the initial reference temperature T_i, the uniform temperature is raised in the whole region to T_f without heat conduction, then the structure buckles due to the thermal effect.

In this case, the temperature field can expressed as [36]:

$$\Delta T = T_f - T_i \tag{23}$$

On the other hand, heat conduction is involved with the coefficient of thermal conduction $K(z)$ varies to the thickness direction z. The property of the conductivity written in terms of z using a power form:

$$K(z,T) = K_m + (K_c - K_m)\left[(2z + h)/2h\right]^k \tag{24}$$

Then, steady-state heat conduction equation and the boundary conditions at the top and bottom surfaces are:

$$\frac{d}{dz}\left[K(z,T)\frac{dT}{dz}\right]=0 \tag{25}$$

in here, $T=T_c$ at $z=h/2$ and $T=T_m$ at $z=-h/2$.

Thus, the solution for temperature distribution across the plate thickness becomes [19]:

$$T=T_c-(T_c-T_m)\frac{\int_{-h/2}^{z}\left(1/K(z,T)\right)dz}{\int_{-h/2}^{h/2}\left(1/K(z,T)\right)dz} \tag{26}$$

An interesting thing is that the formula stands for uniform temperature case for $T_c=T_m$.

3.2. Constitutive equations

Introducing the physical neutral surface at $z=z_0(T)$, and assuming the displace fields as [37]

$$\begin{aligned} u(x,y,z,T)&=u_0(x,y)+\left(z-z_0(T)\right)\phi_x(x,y)\\ v(x,y,z,T)&=v_0(x,y)+\left(z-z_0(T)\right)\phi_y(x,y)\\ w(x,y,z,T)&=w_0(x,y) \end{aligned} \tag{27}$$

where u, v and w are the displacements in the x, y and z direction, while ϕ_x and ϕ_y are the rotations of the normal in the xz and yz planes, respectively.

The constitutive equations can be obtained defined as

$$\begin{Bmatrix} N_b(T) \\ M_b(T) \end{Bmatrix} = \begin{bmatrix} A & B(T) \\ B(T) & D(T) \end{bmatrix} \begin{Bmatrix} \varepsilon_0 \\ \kappa \end{Bmatrix} - \begin{Bmatrix} N_{\Delta T} \\ M_{\Delta T} \end{Bmatrix}$$

$$\left[Q_s(T) \right] = \left[A_s(T) \right] \gamma \tag{28}$$

where $\left[A_s(T) \right] = k_T \left(\int_{-h/2}^{h/2} \frac{E(z,T)}{2\left(1+\nu(T)\right)} dz \right) \begin{bmatrix} 1 & 0 \\ 0 & 1 \end{bmatrix}$

Furthermore, ε_0 and κ are strain vectors based on midpoint and curvature.

in here, $N_b(T)$, $M_b(T)$, $Q_s(T)$, $A_s(T)$ and k_T denote the in-plane force resultant, the moment resultant, the transverse shear force resultant vectors, transverse shear stiffness and temperature-dependent shear correction factor, respectively.

$$
\begin{aligned}
N_b(T) &= \begin{Bmatrix} N_{xx}(T) \\ N_{yy}(T) \\ N_{xy}(T) \end{Bmatrix} = \int_{-h/2}^{h/2} \begin{Bmatrix} \sigma_{xx}(T) \\ \sigma_{yy}(T) \\ \sigma_{zz}(T) \end{Bmatrix} dz \\
M_b(T) &= \begin{Bmatrix} M_{xx}(T) \\ M_{yy}(T) \\ M_{xy}(T) \end{Bmatrix} = \int_{-h/2}^{h/2} (z - z_0(T)) \begin{Bmatrix} \sigma_{xx}(T) \\ \sigma_{yy}(T) \\ \sigma_{zz}(T) \end{Bmatrix} dz \\
Q_s(T) &= \begin{Bmatrix} Q_y(T) \\ Q_x(T) \end{Bmatrix} = \int_{-h/2}^{h/2} \begin{Bmatrix} \sigma_{yz}(T) \\ \sigma_{xz}(T) \end{Bmatrix} dz
\end{aligned}
\tag{29}
$$

On the other hand, A , $B(T)$, $D(T)$ are the in-plane, in-plane bending coupling stiffness and bending stiffness:

$$
\left(A, B(T), D(T)\right) = \int_{-h/2}^{h/2} [E] \left(1, (z - z_0(T)), (z - z_0(T))^2\right) dz \tag{30}
$$

Furthermore, $N_{\Delta T}(T)$ and $M_{\Delta T}(T)$ are the thermal in-plane force resultant and the thermal moment resultant vectors:

$$
\begin{aligned}
\left(N_{\Delta T}(T), M_{\Delta T}(T)\right) &= \begin{pmatrix} N_{\Delta Tx} & M_{\Delta Tx} \\ N_{\Delta Ty} & M_{\Delta Ty} \\ N_{\Delta Txy} & M_{\Delta Txy} \end{pmatrix} \\
&= \int_{-h/2}^{h/2} \left(1, (z - z_0(T))\right) [E] \begin{pmatrix} \alpha(z,T) \\ \alpha(z,T) \\ 0 \end{pmatrix} \Delta T(z) dz
\end{aligned}
\tag{31}
$$

where, the temperature dependent elastic coefficient matrix is:

$$[E]=\frac{E(z,T)}{1-v^2}\begin{bmatrix}1 & v & 0\\ v & 1 & 0\\ 0 & 0 & \dfrac{1-v}{2}\end{bmatrix} \tag{32}$$

3.3. Method of analysis

The principle of virtual work is used to derive the equations of motion:

$$\delta W=\delta W_{\text{int}}-\delta W_{ext}=0 \tag{33}$$

where ∂W_{int} and ∂W_{ext} represent the internal virtual work and the external virtual work, respectively.

$$\begin{aligned}\delta W_{\text{int}} &= \int_V \delta e^T dV=\int_A\left[\delta\varepsilon^T N+\delta\kappa^T M+\delta\gamma^T Q\right]dA\\ &=\delta d^T\left[K^e-K_{\Delta T}+\frac{1}{2}N1+\frac{1}{3}N2\right]d-\delta d^T P_{\Delta T}\end{aligned} \tag{34}$$

In Eq. (26), $d=[u,v,w,\phi_x,\phi_y]^T$ is the displacement vector. In addition, K^e is the global bending stiffness matrix obtained by assembling the A, $B(T)$, $D(T)$ matrix and K^T is the global thermal stiffness matrix in terms of

$N_{\Delta T}(T)$. Also, $N1$, $N2$ and $P_{\Delta T}$ are matrices that denotes the first-order non-linear stiffness, the second-order non-linear stiffness and thermal load vector, respectively.

$$\delta W_{ext} = \delta d^T f = \int_A (P_{air}) \delta w dA = -\delta d^T \{\lambda dA_f + A_d \dot{d}\} \tag{35}$$

Finally, the discredited form of the governing equations of the FGMs plates is obtained as:

$$M\ddot{d} + (\alpha_0 M + \alpha_1 K + \frac{g_a}{\omega_0} A_d)\dot{d} + (K - K_{\Delta T} + \lambda A_f + \frac{1}{2} N1 + \frac{1}{3} N2)d = P_{\Delta T} \tag{36}$$

where the coefficient matrix of $\dot{d}$ represents all the damping effects, the first two terms capture the structural-damping effect and the remaining terms stand for the aerodynamic-damping coefficients [39].

3.4. Solutions of nonlinear method of analysis

The solution of Eq. (28) is assumed as $d = d_s + \Delta d_t$, where d_s and d_t represent the time independent and time dependent solutions, respectively.

Then, two set of coupled governing equations are obtained as:

$$(K - K_{\Delta T} + \lambda A_f + \frac{1}{2} N1_S + \frac{1}{3} N2_S)d_s = P_{\Delta T} \tag{37}$$

and

$$M\ddot{d}_t + (\alpha_0 M + \alpha_1 K + \frac{g_a}{\omega_0} A_d)\dot{d}_t + (K - K_{\Delta T} + \lambda A_f + \frac{1}{2} N1_s + \frac{1}{3} N2_s + N2_{st} + \frac{1}{2} N1_t + \frac{1}{3} N2_t) d_t = 0 \tag{38}$$

where the subscript s and t, represent the static and dynamic states, respectively. Eq. (29) is the equation of motion for static analysis such as a thermal post-buckling analysis. On the other hand, Eq. (30) is the equation of motion for dynamic problem like the vibration behaviors, and then the static equation should be solved before due to they are coupled.

To analyze the thermal post-buckling behavior of the FGMs plates, the incremental form of Eq. (29) is obtained by using the Newton-Raphson iterative method as in Ref. [15].

$$(K - K_{\Delta T} + \lambda A_f + \frac{1}{2} N1_S + \frac{1}{3} N2_S)_i \Delta d_{si+1} = \Delta f_i \tag{39}$$

where the incremental force vector and the updated displacement vector expressed as:

$$\Delta f_f = P_{\Delta T} - (K - K_{\Delta T} + \lambda A_f + \frac{1}{2} N1_s + \frac{1}{3} N2_s)_i d_{si}$$

and

$$d_{si+1} = d_{si} + \Delta d_{si+1}$$

The thermal post-buckling behaviors are calculated repeat until to converged incremental displacement.

The dynamic analysis is employed to obtain the critical conditions for the flutter motion of the model. Assuming a increment in the time dependent solution, Δd_t, the time dependent non-linear stiffness matrices, $N1_t$, $N2_t$ and $N2_{st}$ become zero. Thus equilibrium equation is expressed as:

$$M\Delta\ddot{d}_t + (\alpha_0 M + \alpha_1 K + \frac{g_a}{\omega_0} A_d)\Delta\dot{d}_t + (K - K_{\Delta T} + \lambda A_f + N1_s + N2_s)\Delta d_t = 0 \qquad (40)$$

The solution of Eq.(40) is assumed $\Delta d_t = \varphi_0 e^{\omega t}$ and the degrees of freedom can be reduced by Guyan reduction [40]. Further, φ_0 is a time independent vector, and the plate motion parameter ω is a complex number defined as $\omega = \omega_R + i\omega_I$. Then, the reduced homogeneous equations for eigen analysis with state variables can be written as:

$$\left[\begin{bmatrix} 0 & M_R \\ K_R & C_R \end{bmatrix} - \omega \begin{bmatrix} M_R & 0 \\ 0 & -M_R \end{bmatrix}\right] \begin{Bmatrix} \Delta d_t \\ \Delta\dot{d}_t \end{Bmatrix} = 0 \qquad (41)$$

where M_R, K_R and C_R are the reduced mass, stiffness and damping matrices, respectively.

4. Numerical results and discussions

In this section, numerical results of vibration, buckling and thermal post-buckling behaviors of FGMs are performed as $Si_3N_4 / SUS304$. Elasticity modulus, coefficient of thermal expansion and thermal conductivity for constituent materials listed Table 1 as in Ref. [32]. To obtain the numerical results, 7x7 elements with nine-node model is used for each element, and the results for simply-supported and clamped boundary conditions are investigated. Furthermore, the effect of thermo-micromechanical modeling of the FGMs model is discussed in detail.

The contents of this section are summarized as follows : The first section represents the verification with previous data. The second section shows the vibration and buckling analysis based on thermo-elastic neutral surface and shear correction factor using MTS. Next, thermal post-buckling behaviors of the models based on previous characteristics in thermal environment are studied in the last section.

4.1. Code verification

For the code verification, results are compared with the previous data. Firstly, the homogenized effective material properties of Al / TiC are showed as in Fig. 5 to check with the experimental data of the properties in Ref. [41] for k =1. The evaluated properties in this work using ROM and MTS agree

well with the previous work, and results are quite similar with the experimental data.

Secondly, the initial curve in Fig. 6 shows the non-dimensional shift amount of neutral surface from the mid-plane $\left(z_0 / h\right)$. Specially, the bold line indicates the data for the temperature-independent case. Also, the results present the shift according to volume fraction and the maximum shift is 3.8% from mid-plane of the FGMs model. That is to say, the surface is moved up from the mid-plane. The non-dimensional shift increases as the volume index increase until reaches maximum value. And then, the curve drops down asymptotically from the value. As the elasticity modulus difference is increased, the distance between neutral surface and mid-plane is increased. In the case of $T_{ref} = 300K$, the data is in good agreement with the work in Ref. [18] for the temperature-independent case.

Then, the volume fraction index of maximum value $z_0(T)/h$ ($k_{\max}(T)$) is obtained as [20]:

$$k_{\max}(T) = \sqrt{2\frac{E_c(T)}{E_m(T)}} \tag{42}$$

Maximum value of the shift $k_{\max}$ is 1.76 and is reasonable with the result in Ref. [37].

On the other hand, the shear correction factors are employed to compare the correction factors in Ref. [28] and Ref. [29] without considering the thermo-

elastic effects. Table 2 compares with the literatures, and the results agree well with the data.

Additionally, thermo-elastic vibration behavior of the FGMs structure is investigated. To check layer-wise vibration characteristics, Table 3 shows natural frequencies of the five layers model with clamped-clamped boundary condition with the model is developed using 2 mm for each layer with the length of 125 mm. The data shows good agreements with the results using homogenization method in this work and experimental data. To consider the thermal environments, the fundamental non-dimensional frequency parameters of the model are traced as in Ref. [43]:

$$\Omega_T(T) = \lambda_T(T)\left(\frac{L}{h}\right)^2\sqrt{\frac{\rho_m h^2}{E_m(T)}} \tag{43}$$

Next, the linear thermal buckling is appeared before thermal post-buckling, and then it is necessary to verify linear buckling problem. Thermal buckling temperature of FGMs plate with simply-supported based on neutral surface are verified in Ref. [37].

Lastly, Fig.8 represents thermal post-buckling behavior of FGMs according to reference planes with simply-supported and clamped boundary conditions for $a/h = 1/100$. In the figure, group A, B is simply-supported and clamped boundary conditions, respectively. And also the groups confirm correctly with the results as in Ref. [13].

4.2. Thermo-elastic linear analysis

In this part, thermo-elastic linear analyses of FGMs plate are investigated based on previous temperature-dependent parameters, and results are investigated without aerodynamic effect. Thermal post-buckling behaviors of FGMs plate are investigated, and results are obtained without aerodynamic effect. The temperature is increased continuously by ΔT from $300K$ to $300K + \Delta T$.

4.2.1. Temperature-dependent shear correction factor

Temperature-dependent shear correction factors are presented for Power-law, Exponential, and Sigmoid FGMs models. Furthermore, the neutral surface of the structure is selected as the reference plane. Fig. 9 presents the comparisons of the shear correction factors of the plates for $T_{ref} = 1000K$. The factors are compared the values using ROM with the present works in this figure. From now on, thermo-micromechanical shear correction factors are discussed in detail. As in Fig. 9 (a), the factors are lower than using ROM in the P-FGM type for the volume fraction index *k* lower than 3. An interesting point for the fraction index higher than the value, the factor using MTS is higher than the conventional approach. Furthermore, the factors are increases as the layer number increase. As shown in Fig. 2 (b), the Poisson's ratio based on MTS for high volume fraction has higher value than for ROM. Also, the effective modulus difference between two methods is diminishing for high fraction indices. In this regard, the effect of Poisson's ratio is dominant property of

materials as the effective modulus. Furthermore, MTS always underestimates the shear correction factors than ROM in the S-FGM model. Because the modulus has more dominant effect than Poisson's ratio, the factors vary up to larger value at all times as shown in Fig. 9 (b). Fig. 10 compares the correction factors for P-FGM plate models for layer-wise model. And also, Fig. 11 represents the correction factors for P-, E- and S-FGMs according to temperatures. Fig 11(a) stands for the distribution of the factor for P- model, while the case of S- model shows dissimilar tendency. The data shows an abrupt change, and the maximum difference of the factor is observed for $k = 4$. On the other hand, the curves of the factors for S- model are smoother than P- models as shown in Fig. 11(c). As previously stated, the E- model is described only by an exponential function without the volume fraction index k. That is to say, the micromechanical properties are not applicable to this model. Due to this reason, the factors are significantly influenced by temperature as in Fig. 11(b). As the temperature and the volume fraction index increases, the difference of the factors has higher value.

4.2.2. Vibration and buckling behavior

In this section, thermo-elastic vibration and buckling behaviors of FGMs plate are investigated. The characteristics of the structure in thermal environment are shown in Fig. 12. The plotting lines are non-dimensional fundamental frequencies with temperature difference based on the neutral surface concept. Also, the aspect ratio is fixed $a/h = 60$ because the FSDTP is used. In the figure with $Si_3N_4 / SUS304$, the frequency of the plate is plotted between pure ceramic and metal. However, the decreasing rate of the

frequency is smaller than pure ceramic. Fig. 13 shows the frequency of the model for temperature variation according to the change of the volume fraction index. The natural frequencies are decreased slightly increasing volume fraction index for $\Delta T = 0$, and while $\Delta T = 30$ in Fig. 13 (a), the frequency declines dramatically when the k increases until the minimum point at $k = 1$. Therefore, volume fraction ranges before thermal buckling point are decreased with increase of temperature. Fig. 13 (b) shows the distribution of frequencies to be same with Fig. 13 (a). However, the temperature variations with clamped condition are larger than simply-supported model due to the clamped condition is affected by temperature lower than the simply-supported condition. To consider the interaction of particles in the model, MTS are also studied for thermo-elastic vibration in thermal environment.

Table 4 presents the effect of reference plane and MTS on the thermal buckling behavior under uniform temperature rise status. It shows that the buckling temperature decreases by using neutral surface to the reference plane, increases by using MTS. The results are due to reducing elasticity modulus using the homogenization scheme only. That is to say, the model using the scheme is influenced by thermal environment less than the conventional method.

4.3. Aerothermo-elastic nonlinear analysis

4.3.1. Stability Boundary

Fig. 14 depicts stability boundary of all clamped rectangular $\mathrm{SUS304}/Si_3N_4$ FGM panel with non-linear temperature rise condition. At the region 'A' in this figure, the panels are flat ($d_s = 0$) and both statically and dynamically stable. The region 'B' is defined by aerodynamic thermal post-buckling analysis and the boundaries between the regions 'A' and 'B' indicate critical conditions where bifurcation buckling occurs. The panel is buckled ($d_s \neq 0$) but dynamically stable in the region 'B'. The region 'C' represents dynamically unstable region where flutter occurs. In this region, a panel oscillates from its static equilibrium position with a self-exited harmonic motion. The dynamic stability boundaries which lie between the regions 'A' and 'C' can be defined by linear flutter analysis. The region 'D' is a chaotic region and Eqn. (37) does not give a convergent solution d_s, i.e. d_s is undetermined and snap-through or chaotic motion happens in this region. From this figure, it is noted that both the critical aerodynamic pressures for panel flutter and the critical temperature for thermal buckling increase, as the volume fraction index decreases.

4.3.2. Thermal post-buckling

In this section, thermal post-buckling characteristics of FGMs plate are investigated without heat transfer effect. The thermal conduction are gradually changed by temperature metal to ceramic for thickness direction. Fig. 15

indicates the non-dimensional center deflection in thermal post-buckling behavior. It is interesting thing that the temperature difference for snap-through is increases as the number of layer increases. This is because stair distribution of material properties affects the behavior.

From now on, neutral surface shifts are discussed for Si_3N_4 / $SUS304$ with temperature dependent material properties. Fig. 16 depicts the effect of the position of neutral surface and homogenized properties according to temperature variations for the clamped-clamped condition. Fig. 16 (b) shows the heat conduction effects compared with Fig. 16 (a). In the case with heat conduction, the bifurcation point is appeared at higher temperature than the uniform temperature rise condition. Furthermore, the interesting thing is that k increases, then the difference of the deviation amount also increased. Therefore, neutral surface are applied in thermal post-buckling analysis due to asymmetric of material property.

For using homogenized properties, Fig. 17 depicts the result considering heat transfer effects. In the figure, the snap-through point is appeared earlier than previous model as using rule of mixture method, and the model moves to up-side direction slowly. Furthermore, the bifurcation can be occurred slowly than the previous model regardless of volume fraction. As compare Fig. 16 and Fig. 17, distributions of plate are differ from each condition, and then homogenized heat conduction affects highly than other effective material properties for thermal post-buckling behavior.

5. Conclusions

In this paper, temperature-dependent modeling of Functionally Graded Materials (FGMs) plate are studied for thermo-elastic vibration, buckling and thermal post-buckling with the micro-mechanical properties. And thermo-micromechanical modified shear correction factors are used for crucial evaluation to compensate the shear stress effects in thermal environments. Layer-wise modeled FGMs plates are investigated in the thermo-mechanical environment and it is more actual method to approach practical analysis. Based on the First-order Shear Deformation Theory of Plate (FSDTP), the equilibrium and stability equations of functionally graded rectangular plates have been derived. To verify the accuracy of the present theory, the results obtained by the present analysis have been compared with their counterparts in the literature. The homogenized properties of the FGMs plates are calculated using homogeneous scheme such as Rule of Mixture (ROM) and the Mori-Tanaka Scheme (MTS) based on neutral surface. Furthermore, concept of homogenization scheme is used for advanced results, and the difference of the properties obtained based on ROM and MTS are performed in detail. And then, the neutral surface positions are revealed with various conditions such as volume fraction and temperature, and the comparisons of the reference plane are investigated using temperature-dependent material properties. Also, the thermo-micromechanical shear correction factors are proposed for the model. Basically, the factors are determined using the neutral surface concept in the thermal environment of the structures. The numerical results are presented and the data are compared with the cases for ROM and

MTS for the three-type models. Specifically, the shear correction factors depend on three variables such as the ratio between the effective properties of ceramic and metal, the volume fraction index and the thermo-micromechanical properties. As the fraction index increases gradually, the factors of the S-type model varies smoother than P-type model. Although the E-type model is independent of the fraction index, the effect of reference temperature is observed. Then, as the temperature increases, the thermal effect also increases. In the homogenization approach, the factors are also changed due to effective properties such as Young's modulus and Poisson's ratio. More generally, the micromechanical properties make the estimation of stress concentration lower than macroscopic case. Also, linear analyses like vibration and buckling behaviors are reviewed considering homogenized properties based on neutral surface. Thermo-elastic parameters and the properties using MTS affects the behaviors as previously stated. As shown in thermal post-buckling results, the snap-through point are occurred early from equilibrium point using neutral surface concept, and the deflections are almost the same results for all clamped boundary conditions of models. The center position with homogenized properties moves to down-side faster than previous model as temperature increase, and snap-through are delayed from equilibrium point due to the properties decrease the stiffness. The bifurcation point is appeared early in the case using MTS, and the symmetric deflection of the model with homogenized properties is restored faster than previous model based on neutral surface. For considering heat transfer effects, the snap-through point is occurred earlier than previous model as using ROM, and the bifurcation can be occurred slowly than the previous model regardless of

volume fraction with clamped boundary condition. The distributions of plate are differ from each condition, and then homogenized heat conduction affects higher than other effective material properties for thermal post-buckling behavior. In the layer-wise model, also the micromechanical properties make the estimation of thermal effects lower than macroscopic case. And then, the effects are lower as the number of layer is decrease, while the convergence is showed as the number increases.

The flutter analysis and limit-cycle oscillation for the step-wise FGMs plate based on temperature-dependent parameters are investigated as a future work. The parameters are affects limit-cycle oscillation more than static analysis. Specially, thermo-micromechanical shear correction factor of layer-wise model is important point for more actual analysis in thermal environments for FSDTP.

References

[1] M. Niino, T. Hirai and R. Watanabe, "The functionally gradient materials", Journal Japan Soc. Composite Materia, vol 13, pp. 257-264.

[2] Y. Miyamoto, W. A. Kaysser, B. H. Rabin, A. Kawasaki and Renee G. Ford, "Functionally Graded Materials: Design, Processing and Applications," Kluwer Academic Publishers, Boston, 1999, pp. 1-6.

[3] M. Bouazza, A. Tounsi, E. A. Adda-Bedia and A. Megueni, "Thermoelastic Stability Analysis of Functionally Graded Plates: An Analytical Approach", Computer Material Science, 2010; 49: 865–870.

[4] M. B. Bouiadjra, M. S. Ahmed Houari and A. Tounsi, "Thermal buckling of functionally graded plates according to a four-variable refined plate theory", Journal of Thermal Stresses, 2012;35: 677–694.

[5] S. R. Li, J. H. Zhang and Y. G. Zhao, "Thermal post-buckling of functionally graded material Timoshenko beams", Applied Mathematics and Mechanics, 2006, vol. 27, pp. 803-810.

[6] T. Prakash, M. K. Singha and M. Ganapathi, "Thermal postbuckling analysis of FGM skew plates", Engineering Structures, 2008, vol30, pp 22-32.

[7] H. S. Shen, "Thermal postbuckling behavior of shear deformable FGM plates with temperature-dependent properties", International Journal of

Mechanical Sciences, 2007, vol. 49, pp. 466-478.

[8] S. L. Lee and J. H. Kim, "Thermal post-buckling and limit-cycle oscillation of functionally graded panel with structural damping in supersonic airflow", Composite Structure, 2009, vol.91, pp. 205-211.

[9] C. Y. Lee and J. H. Kim, "Thermal post-buckling and snap-through instabilities of FGM panels in hypersonic flows", Aerospace Science and Technology, 30(2013) 175-182.

[10] Achchhe Lal, K. R. Jagtap and B.N. Singh, "Post buckling response of functionally graded materials plates subjected to mechanical and thermal loadings with random material properties", Applied Mathematical Modeling, 2013 vol.37, pp. 2900-2920.

[11] K. M. Liew, J. Yang and S. Kitipornchai, "Thermal post-buckling of laminated plates comprising functionally graded materials with temperature-dependent properties", Journal of Applied Mechanics, 2004,vol.71, pp. 839-850.

[12] H. M. Navazi and H. Haddapour, "Aero-thermoelastic stability of functionally graded plates", Composite Structure ,2007, vol. 80, pp. 580-587.

[13] K. J. Sohn and J. H. Kim "Structural stability of functionally graded panels subjected to aero-thermal loads", Composite Structures, 2008, vol. 82, pp. 317-325.

[14] T. Prakash and M. Ganapathi, "Supersonic flutter characteristics of

functionally graded flat panels including thermal effects", Composite Structures, 2006, vol. 72, pp.10-18.

[15] I. Lee, D.M. Lee and I. K. Oh, "Supersonic flutter analysis of stiffened laminated plates subject to thermal load", Journal of Sound and Vibration, 1999;,vol. 224, pp. 49-67.

[16] H. H. Ibrahim, M. Tawfik and M. Al-Ajmi, "Thermal buckling and nonlinear flutter behavior of functionally graded materials panels", Journal of Aircraft, 2007, vol. 44, pp. 1610-1618.

[17] H. Haddadpour, H. M. Navazi and F. Shadmehri. "Nonlinear oscillation of a fluttering functionally graded plates, Composite Structures, 2007, vol. 72, pp. 242-250.

[18] T. Prakash, M.K. Singha and M. Ganapathi, "Influence of neutral surface position on the nonlinear stability behavior of functionally graded plates", Computer Mechanics, 2008, vol. 43, pp. 341-350.

[19] D.G. Zhang, Modeling and analysis of FGM rectangular plates based on physical neutral surface and high order shear deformation theory, International Journal of Mechanic Science, 2013, vol. 68, pp. 92–104.

[20] H. Yaghoobi and A. Fereidoon, "Influence of neutral position on deflection of functionally graded beam under uniformly distributed", World Applied Science Journal, 2010, vol. 10, pp.337-341.

[21] T. Mori and K. Tanaka, "average stress in matrix and average elastic energy of materials with mis-fitting inclusions". Acta Metall Mater, 1973, vol. 21, pp. 571-574.

[22] H.S. Shen and Z.X. Wang, "Assessment of Voigt and Mori-Tanaka models for vibration analysis of functionally graded plates", Composite Structures, 2013, vol.47, pp. 90-104.

[23] Y. Kiani and M. R. Eslami, "Thermal post-buckling of imperfect circular FGM plates: examination of Voigt, Mori-tanaka and self-consistent schemes", J Press Vessel Technol (2014), http://dx.doi.org/10.1115/1.4026993.

[24] A. H. Akbarzadeh, A. Abedini and Z. T. Chen, "Effect of micromechnical models on strucutral responses of functionally graded plates", Composite Structure, 2015, vol. 119, pp. 598-609.

[25] Stefanos Vlachoutsis. Shear correction factors for plates and shells. J Numer meth Eng 1992;33:1537-52.

[26] Madabhusi-Raman P, Davalos JF. Static shear correction factor for laminated rectangular beams. Compos Part B: Eng 1996;27(3-4);285-93.

[27] Birman V, Bert CW. On the Choice of Shear Correction Factor in Sandwich Structures. J Sandw Struct Mater 2002;4(1):83-95.

[28] Nguyen TK, Karam Sab. Shear Correction Factors for Functionally Graded Plates, J Mech Adv Mater Struct 2007;14:567-75.

[29] Menaa R, Tounsi A, Mouaici F, Mechab I, Zidi M, Bedia EA. Analytical Solutions for Static Shear Correction Factor of Functionally

Graded Rectangular Beams. J Mech Adv Mater Struct 2012;19(8):641-52.

[30] Lim T-K, Kim J-H. Thermo-elastic effects on shear correction factors for functionally graded beam. Compos Part B: Eng 2017;123;262-70.

[31] Lim T-K, Kim J-H. Temperature-dependent shear correction factors with micromechanical properties for FGM plates. Compos Part B: Eng 2017;submitted.

[32] J.N. Reddy and C.D. Chin, "Thermo-mechanical analysis of functionally graded cylinders and plates", Journal of Thermal Stresses, 21:6 593-626.

[33] D.G. Zhang and Y.H, Zhou. "A theoretical analysis of FGM thin plates based on physical neutral surface", Computer Material Science, 2008, vol. 44, pp. 716-720.

[34] B.W. Rosen and Z. Hashin, "Effective thermal expansion coefficients and specific heats of composite materials", International Journal of Engineering Science, 1970, vol. 8, pp. 157–173.

[35] H. Hatta and M. Taya, "Effective thermal conductivity of a misoriented short fiber composite", Journal of Applied Physic, 1985, vol. 58, pp.2478–2486.

[36] R. Javaheri and M. R Eslami, "Thermal buckling of functionally graded plates". AIAA Journal , 2002, vol. 40, pp.162–169.

[37] Y. H. Lee, S. I. Bae and J. H. Kim, “Thermal buckling behavior of

functionally graded plates based on neutral surface", Composite Structure, 2016, vol. 137, pp. 208-214.

[38] E. Efraim and M. Eisenberger, "M. Exact vibration analysis of variable thickness annular isotropic and FGM plates". Journal of Sound Vibration, 2007, vol. 299,pp. 720-38.

[39] D. A. R. Mohammad, N. U. Khan and V. Ramamurti, "On the role of Rayleigh damping", Journal of Sound Vibration, 1995, vol. 185, pp. 207-218.

[40] R. D. Cook, D. S. Malkus, M. E. Plesha and R.J. Witt, "Concept and applications of finite element analysis", New York: John Wiley & Sons; 2002.

[41] P. C. Zhai, C.R. Jiang, Q. J. Zhang, J. B. Holt, M. Koizumi, T. Hirai and Z. A. Munir, editors. "Ceramic Transactions: Functionally Gradient Materials", Westerville: The American Ceramic Society; 1993, pp. 449.

[42] C. Y. Lee and J. H. Kim, "Evaluation of homogenized effective properties for FGM panels in aero-thermal environments", Composite Structures, 2015,vol.120, pp. 442-450.

[43] Wattanasakulpong N, Prusty BG, Kelly DW, Hoffman M. Free vibration analysis of layered functionally graded beams with experimental validation. Mater Des 2012;36:182-90.

Table 1
Material properties of metal and ceramic [32]

Properties		P_{-1}	P_0	P_1	P_2	P_3
Si_3N_4	$E(Pa)$	0	348.4e9	-3.070e-4	2.16e-7	-8.946e-11
	$\alpha(1/K)$	0	5.87e-6	9.09e-4	0	0
	$k(W/mK)$	0	13.723	-1.032e-3	5.46e-7	-7.876e-11
	ν	0	0.24	0	0	0
$SUS304$	$E(Pa)$	0	201.04e9	3.079e-4	-6.53e-7	0
	$\alpha(1/K)$	0	12.33e-6	8.086e-4	0	0
	$k(W/mK)$	0	15.379	-1.264e-3	2.09e-6	-7.223e-10
	ν	0	0.3262	0	0	0

Table 2
Comparison of shear correction factors

Aluminum-SiC			
k	Menaa et al.[29]	Nguyen et al.[28]	Present method
0.2	0.8439	0.8440	0.8438
1	0.8305	0.8305	0.8299
4	0.6784	0.6786	0.6775
8	0.6637	0.6634	0.6628
10	0.6746	0.6743	0.6736

Table 3

Natural frequencies of five-layer FGMs beam under clamped-clamped boundary condition

Mode	Frequency (Hz)		
	ROM [43]	Expt [43]	Present
1	1546.14	1433	1427.25
2	9103.2	8422	8375.15
3	20209.55	18388	18275.78
4	23500.77	21589	21369.74

Table 4
Comparison of buckling temperatures for k=1

a/h	20	60	100
Mid-surface	2.79E+02	31.41	11.32
Neutral-surface	2.76E+02	31.08	11.20
Mori-Tanaka scheme	2.80E+02	31.51	11.35

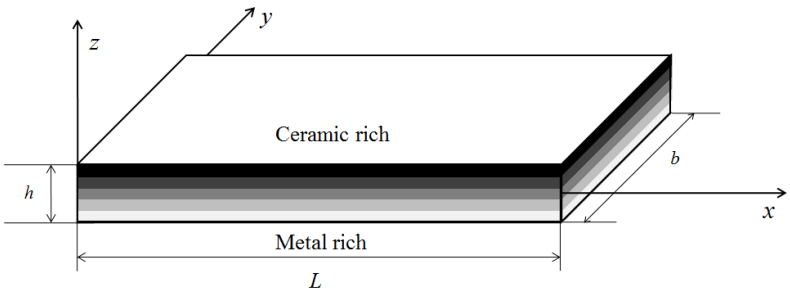

Fig. 1. A layer-wise FGM plate model

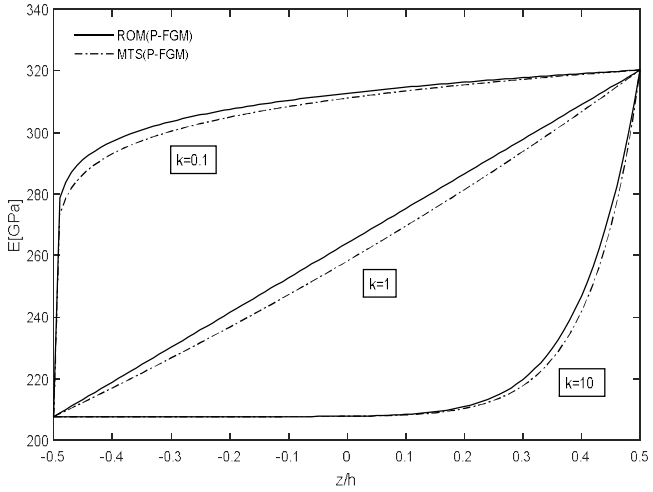

(a)

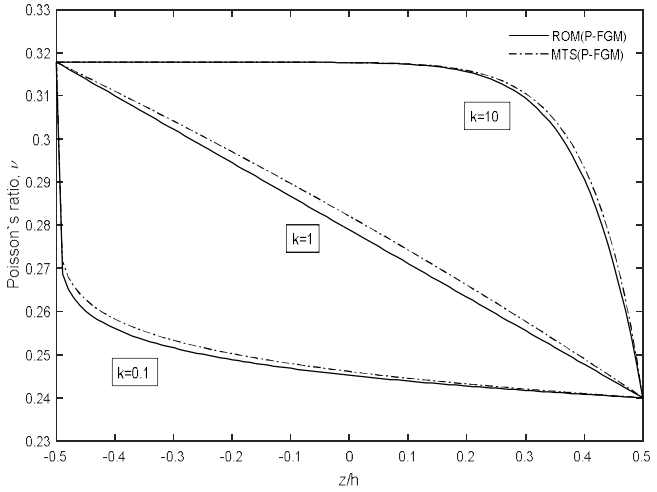

(b)

Fig. 2. Effective properties of P-FGM through the thickness distribution

(a) Young's modulus; (b) Poisson's ratio

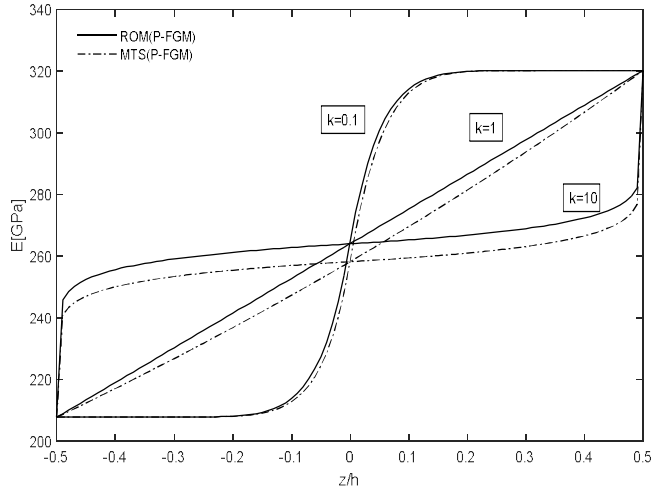

(a)

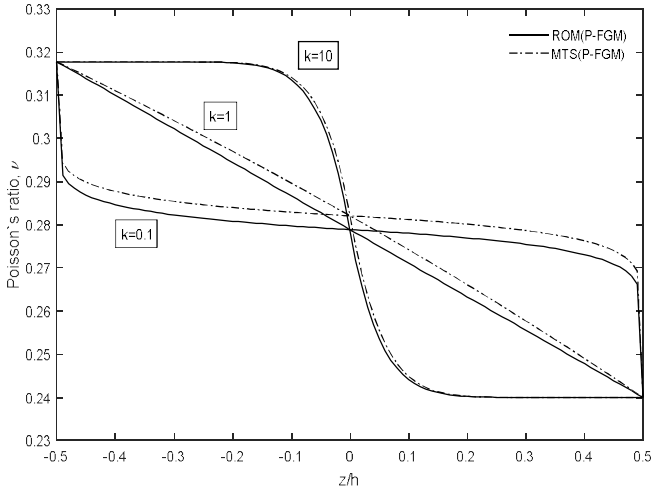

(b)

Fig. 3. Effective properties of S-FGM through the thickness distribution

(a) Young's modulus; (b) Poisson's ratio

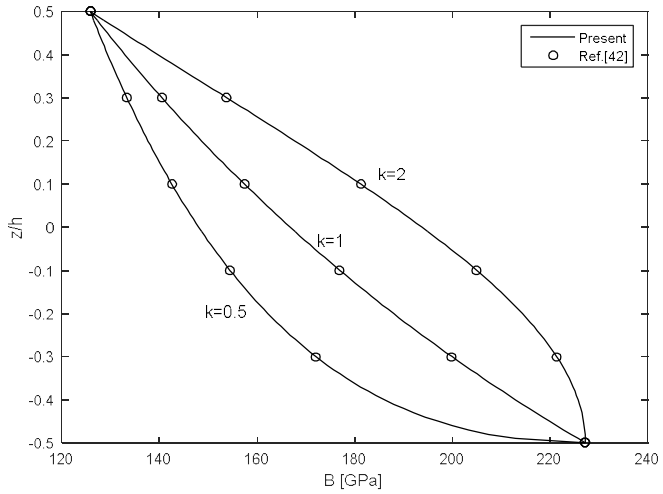

(a)

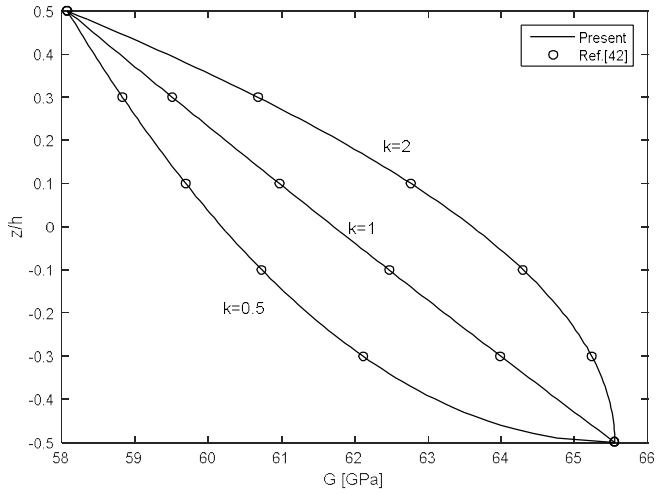

(b)

Fig. 4. Homogenized modulus of FGMs plate
(a) Bulk modulus ; (b) Shear modulus

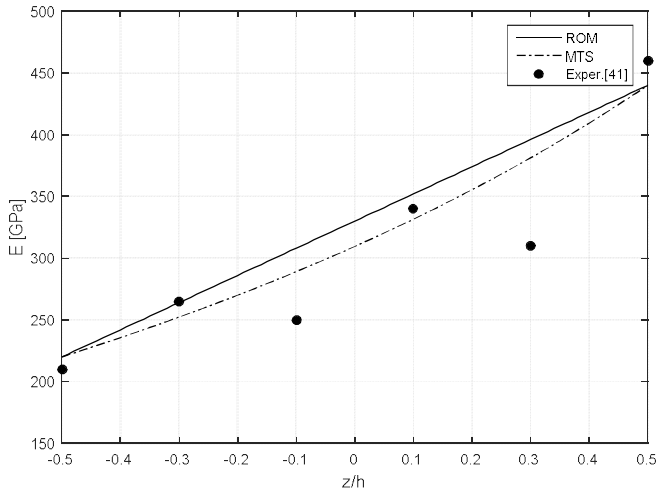

(a)

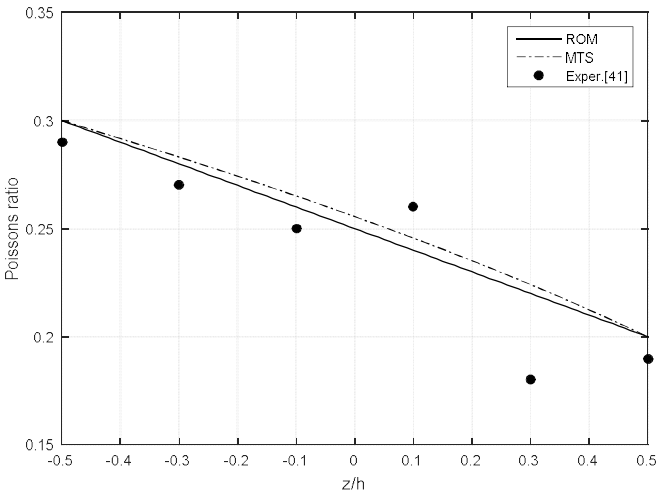

(b)

Fig. 5. Comparison of effective properties
(a) Young's modulus; (b) Poisson's ratio

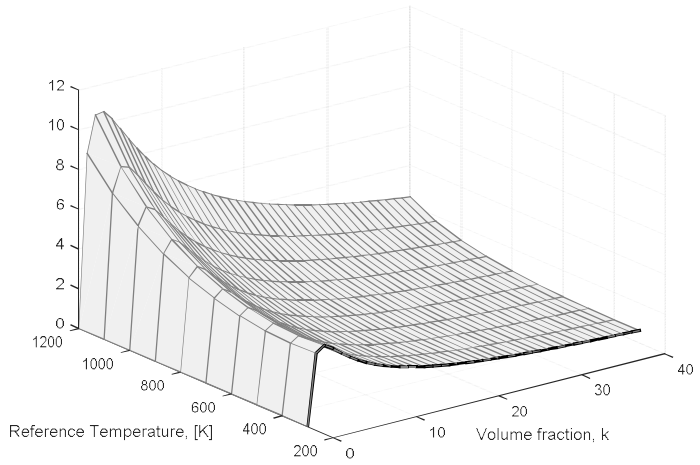

Fig. 6. Non-dimensional neutral surface position from mid-plane

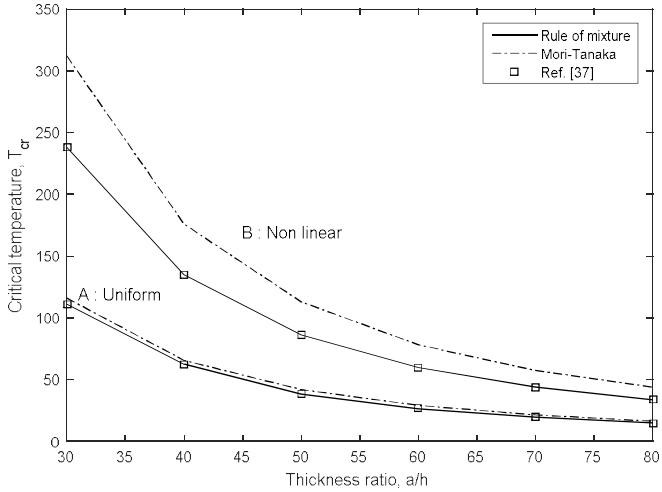

(a)

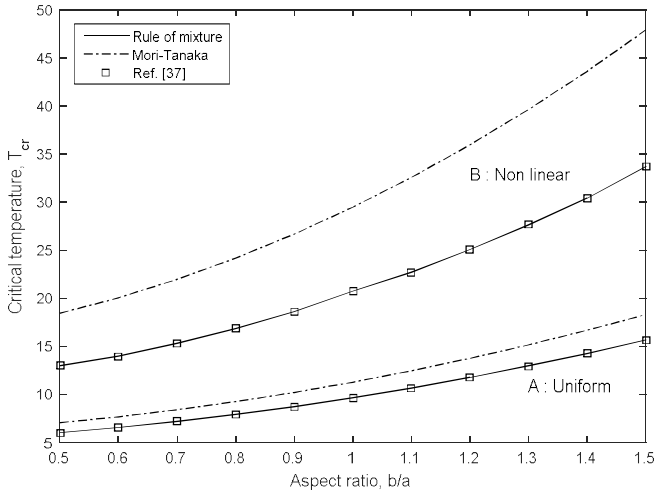

(b)

Fig. 7. Critical temperature based on neutral surface
(a)Thickness; (b) Aspect ratio

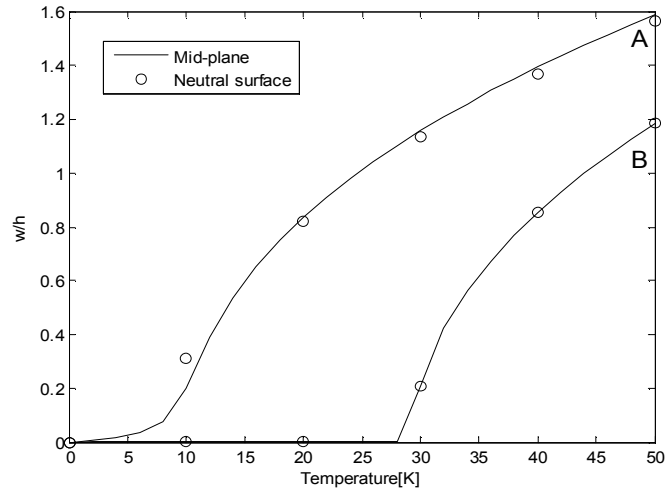

Fig. 8. Non-dimensional center deflections for mid-plane and neutral surface

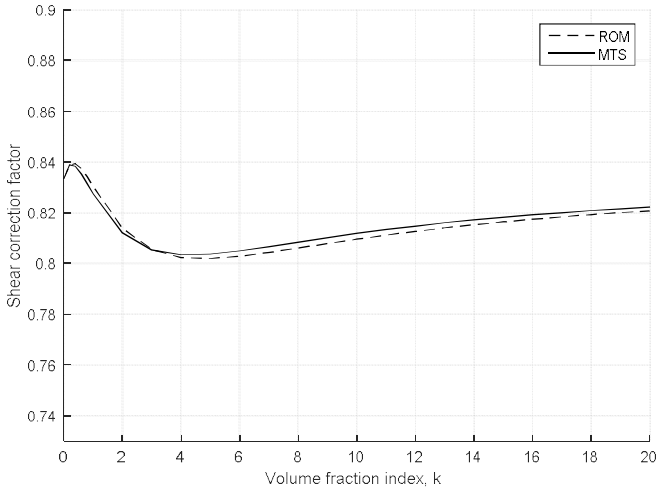

(a)

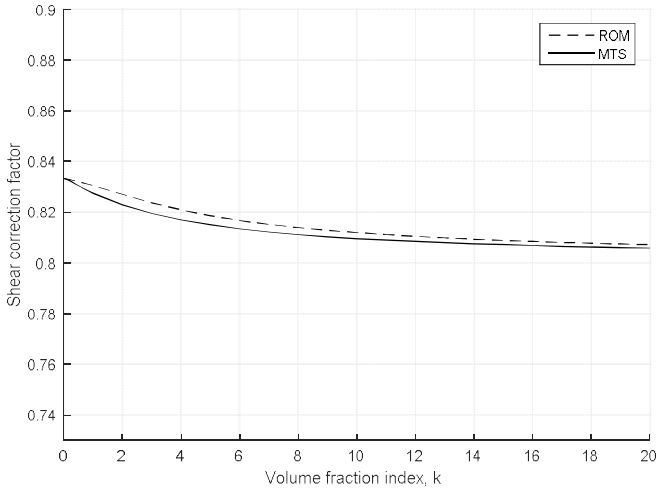

(b)

Fig. 9. Comparisons of the shear correction factor of Si_3N_4 /SUS304 FGMs plate
(a) P-FGM; (b) S-FGM

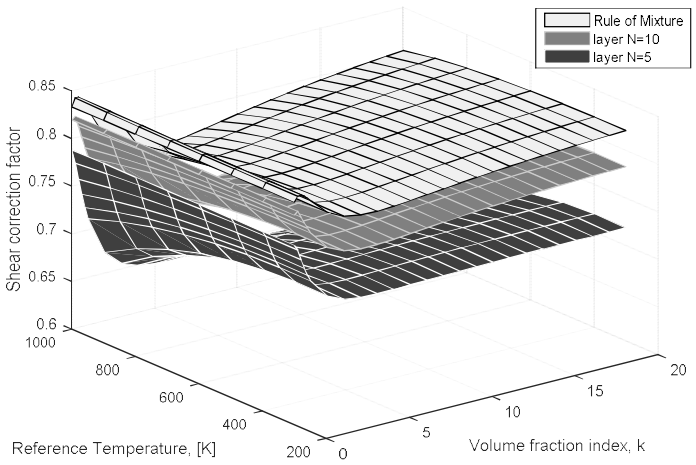

Fig. 10. Comparisons of the shear correction factor for layer-wise model

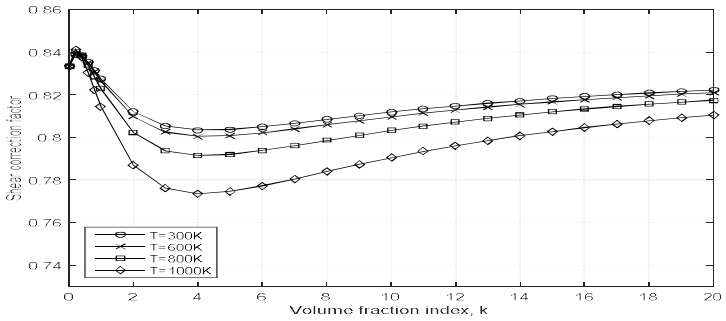

(a)

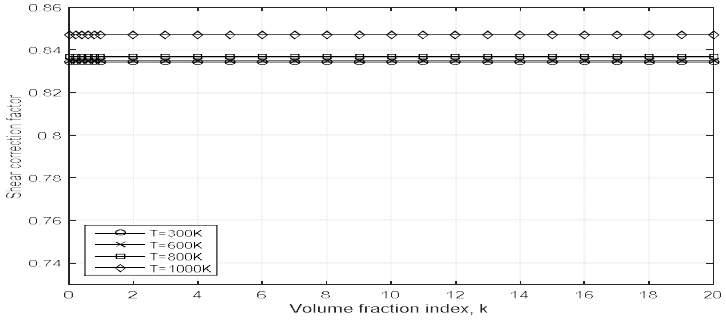

(b)

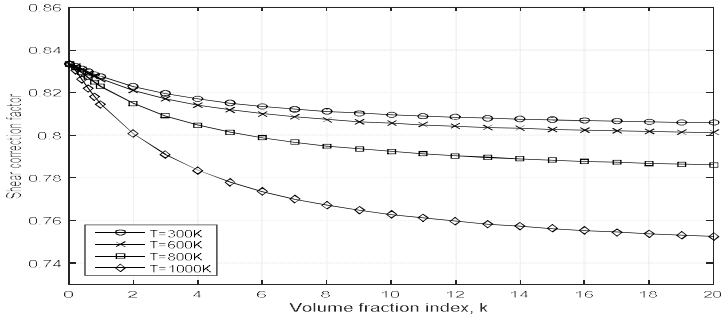

(c)

Fig. 11. Comparisons of the shear correction factor for increasing temperature
(a) P-FGM; (b) E-FGM; (c) S-FGM

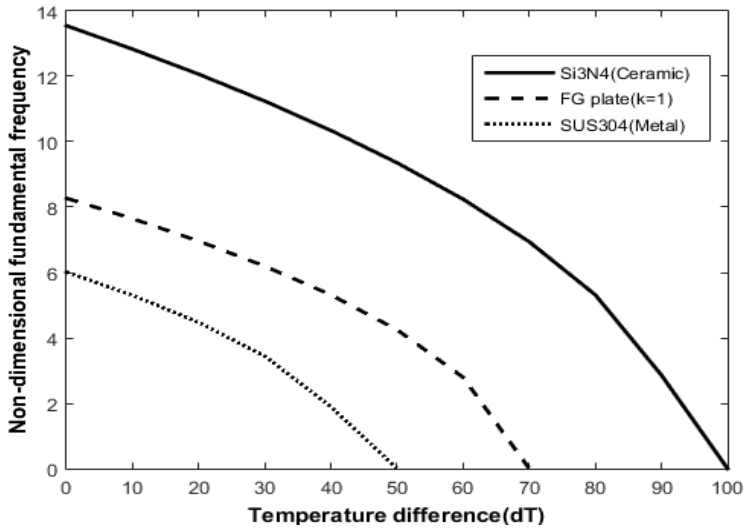

Fig. 12. Non-dimension fundamental frequency of simply-supported FGMs plates

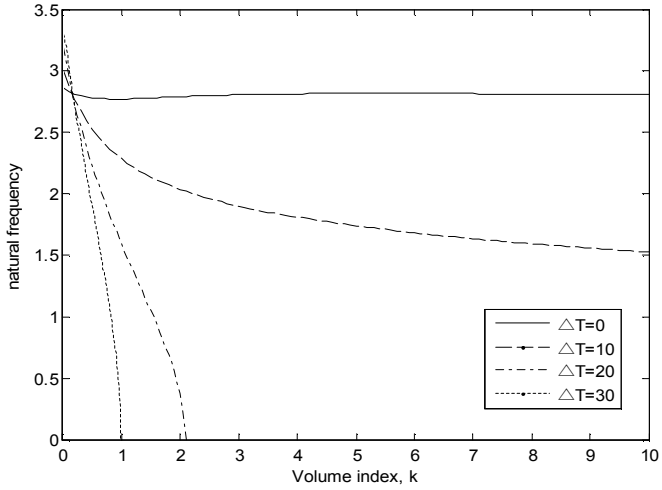

(a)

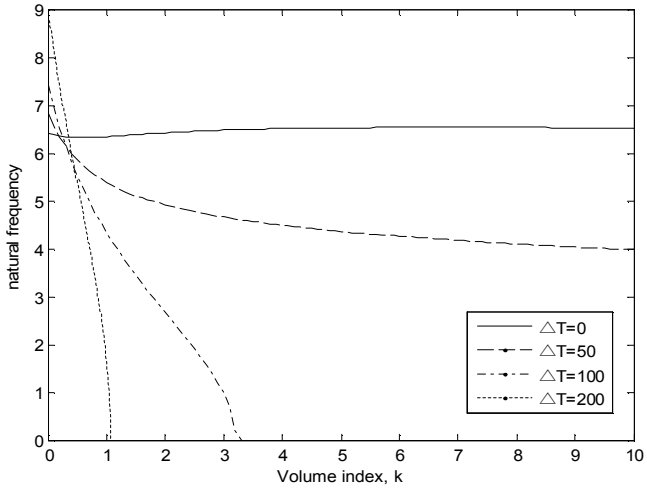

(b)

Fig. 13. Frequencies of thermal model according to volume index

(a) Simply-supported; (b) Clamped

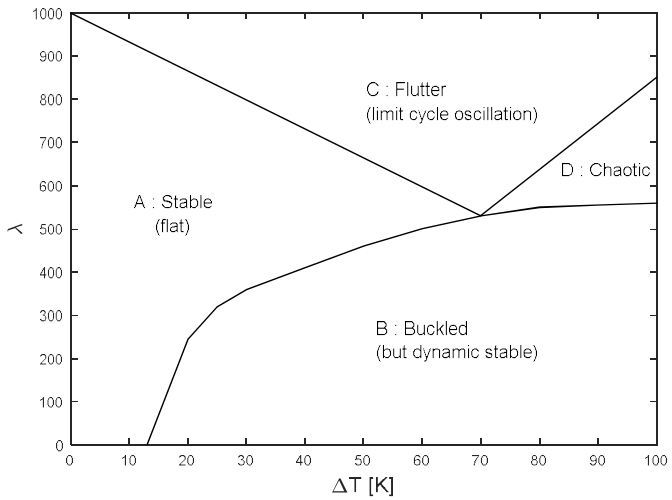

Fig. 14. Stability boundary of FGMs plate

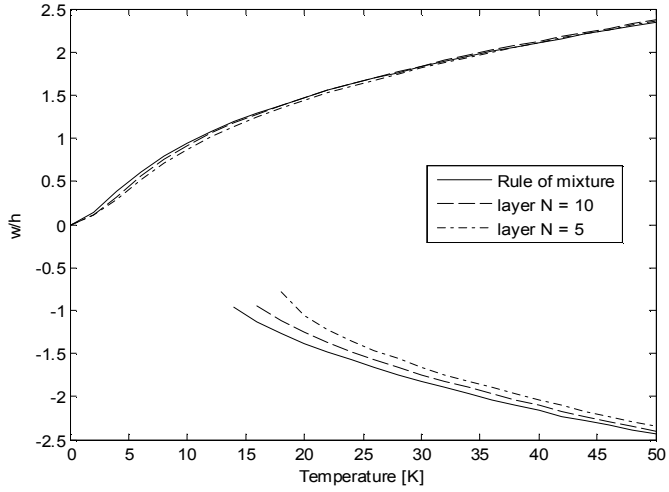

Fig. 15. Non-dimensional center deflections for layer-wise model

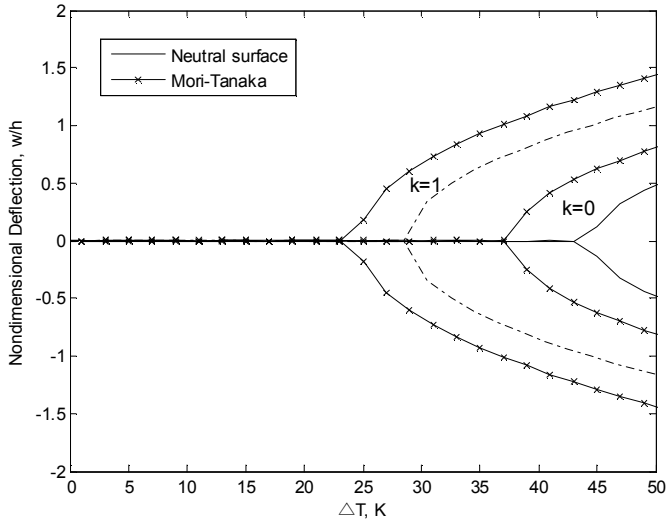

(a)

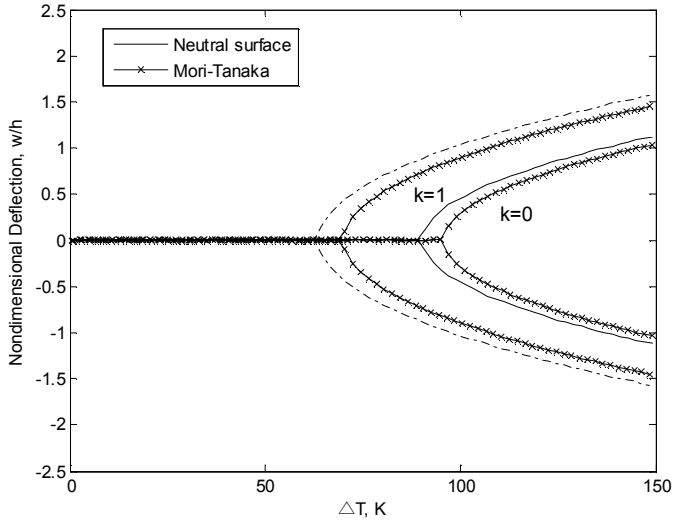

(b)

Fig. 16. Non-dimensional center deflection according to reference plane ($\Delta T = 300K + \Delta T$)
(a) Uniform temperature ; (b) Heat transfer

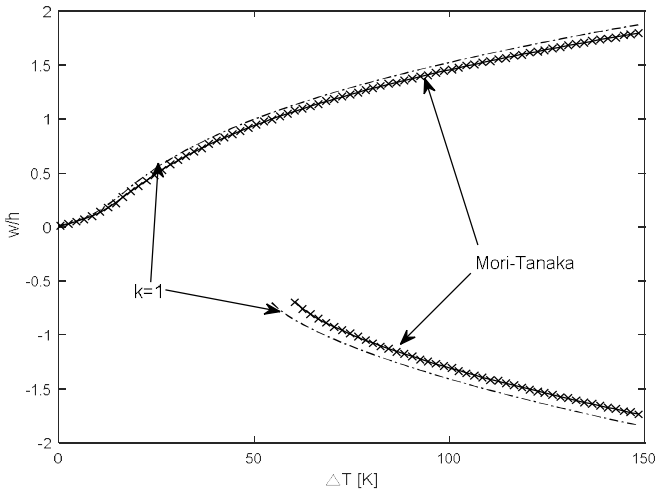

Fig. 17. Non-dimensional center deflection according to reference plane ($\Delta T = 300K + \Delta T$)

국 문 초 록

경사기능재료는 우주 항공, 자동차 및 상업용 구조물 등의 고온 영역에서 진보된 구조재료로서 사용되어왔다. 본 연구는 경사기능재료 에 대한 열탄성 진동 및 후좌굴 거동에 대해 연구하였다. 그리고 열 미소기계적 물성으로 발전된 전단보정계수는 열 환경에서의 전단 응력 효과를 보상하기 위해 중요하게 다루어진다. 열 기계적 환경에서 층 모델링된 경사기능재료 판을 연구하였다. 분석을 위해서 1 차 전단이론과 미소기계적 물성이 함께 사용된다. 그리고 재료는 한 쪽 면에서 다른 쪽 표면으로 연속적인 변화를 갖는 물성값을 가진다. 물성값은 온도에 의존적이며, 경사기능재료의 두께 방향 비대칭성으로 인해 기존에 사용된 중앙면이 아닌 중립면을 기준면으로 채택하였다. 또한, 열적 조건에서 경사기능재료의 균질화 모델링을 도입하며, 이 방법은 해석에 있어서 더 실제적인 방법이 된다. 균질화 기법 중에서도 분자 상호 작용을 고려한 Mori-Tanaka 방법을 채택하였는데, 이 방법은 체적, 전단 탄성률을 통하여 균질화된 물성치를 구해낸다.

지배방정식은 1 차 전단이론을 기초로 구조적 비선형성을 고려하기 위해 von Karman 변형률-변위 관계를 적용하여 이끌어냈다. 나아가 열적 후좌굴을 해석하기 위해 Newton-Raphson 방법을 적용하였다. 모델링 기법을 다양하게 적용하여 기존 연구와 비교하였다. 균질화된 모델의 중립면 효과가 열탄성 환경에서 진동 및 후좌굴 행동에 미치는 영향을 분석하였다.

주요어 : 경사기능 재료, 전단 보정 계수, 진동, 열적 후좌굴, 중립면, 모리-다나카 방법

학 번 : 2015-22737